Results in Physics 66 (2024) 108004

Contents lists available at ScienceDirect

Results in Physics

journal homepage: www.elsevier.com/locate/rinp

Ultra-sensitivity of surface plasmon resonance sensor using halide perovskite $FASnI_3$ and 2D materials on Cu thin films

H. Bouandas [a], Y. Slimani [b], A. Bakhouche [a], N. Bioud [c,d], A. Djemli [e,f], Faisal Katib Alanazi [g,*], I. Bouchama [h], M.A. Ghebouli [h,i], M. Fatmi [h,*], T. Chihi [h]

[a] Applied Optics Laboratory, Institute of Optics and Precision Mechanics, University Setif 1, Setif 19000, Algeria
[b] Laboratory of Intelligent System, Faculty of Technology, University Ferhat Abbas Setif 1, Setif 19000, Algeria
[c] Faculty of Sciences and Technology, University of Mohamed El Bachir El Ibrahimi-Bordj Bou Arreridj, 34000, Bordj Bou Arreridj, Algeria
[d] Laboratory of Optoelectronic and Compounds, Faculty of Sciences, University of Setif 1, 19000 Setif, Algeria
[e] Faculty of Physics, University of Sciences & Technology Houari Boumediene (U.S.T.H.B), El Alia, BP 32, Bab Ezzouar 16111, Algiers, Algeria
[f] Physics and Chemistry of Materials Lab, Department of Physics, University Mohamed Boudiaf of M'sila, 28000, M'sila, Algeria
[g] Department of Physics, College of Sciences, Northern Border University, Arar 73222, Saudi Arabia
[h] Research Unit on Emerging Materials (RUEM), University Ferhat Abbas of Setif 1, Setif 19000, Algeria
[i] Department of Chemistry, Faculty of Sciences, University Mohamed Boudiaf of M'sila, 28000 M'sila, Algeria

ARTICLE INFO

Keywords:
Surface plasmon resonance
Biosensor
Halide Perovskite ($FASnI_3$)
2D materials
Sensitivity
Transfer matrix method

ABSTRACT

This paper studies a novel surface plasmon resonance (SPR) biosensor using a BK7 glass prism, a copper (Cu) metal plasmonic layer, which combine a halide perovskite (FASnI3) with two-dimensional (2D) materials such as phosphorus black, graphene and TMDC (MoS_2, $MoSe_2$, WS_2, WSe_2) for the detection of breast cancer cells. We have optimized the thickness of each layer in order to obtain maximum sensitivity. A numerical study mainly uses the transfer matrix principle, while the attenuation total reflection method involves examining the reflection properties. The evaluation of SPR biosensor configurations serves to obtain optimal performance. The simulation results indicate that the integration of halide perovskite (FASnI3) and 2D materials into the BK7/Cu/medium sensing structure significantly improves the sensitivity and figure of merit (ZT). The outstanding results in terms of sensor performance characteristics are observed in the BK7/Cu (48 nm)/FASnI3 (5 nm)/BP (0.53 nm) configuration. The figure of merit and sensitivity estimated at 123.11 RIU^{-1} and 459.28°/RIU, with a notable improvement of 338.45 %.

Introduction

Surface Plasmon Resonance (SPR) sensors, in particular, have emerged as pivotal tools due to their unique characteristics such as fast detection ability in real time, quick response and high sensitivity to changes in the refractive index near the sensor surface [1]. SPR biosensors hold significant potential in biomedical research, such as medical detection of human blood [2], bacteria detection [3] and SPRs are extensively utilized in designed for cancer cell [4]. The rapid advancement in biosensor technology has significantly enhanced the early detection capabilities for various diseases, including cancer. A noteworthy study demonstrated the potential of a multi-layered Kretschmann configuration-based on refractive index sensor for cancer detection, illustrating the substantial impact of such configurations on diagnostic capabilities [5]. In the same context, high-performance biosensors based on angular plasmonic effects in multilayer designs show remarkable improvements in sensitivity, for a part of new materials to improve one-dimensional designs [6]. SPR sensors typically use two coupling configurations in a prism, the Otto [7] and Kretschmann configurations [8]. The Kretschmann configuration is preferred when plane-polarized light in the visible range incident on a metal surface couples with the prism using an angle interrogation technique [9]. This configuration, combined with attenuated total reflection spectroscopy, excites a larger number of surfaces plasmons at the prism-dielectric interface [10]. Utilizing the Kretschmann configuration with angular interrogation and a single laser light source yields the highest signal-to-noise ratio (SNR), thereby enhancing SPR sensor performance [11–13]. Generally, common metals used in SPR sensors include Silver (Ag),

* Corresponding authors.
E-mail addresses: Faisal.katib.al@gmail.com (F. Katib Alanazi), fatmimessaoud@yahoo.fr (M. Fatmi).

https://doi.org/10.1016/j.rinp.2024.108004
Received 18 August 2024; Received in revised form 24 September 2024; Accepted 6 October 2024
Available online 24 October 2024

Aluminum (Al), Gold (Au), Copper (Cu), and Indium (In). While gold is favored for its stability and bioactivity, it produces a broader SPR curve, which impacts sensor sensitivity [14,15]. Silver offers better performance due to its narrower resonance peak, enhancing accuracy and sensitivity [16,17]. However, silver's propensity for oxidation and corrosion necessitates the use of bimetallic layers to protect it and enhance sensitivity [18]. As the second most conductive substance after silver, copper (Cu) is significantly less expensive than gold and silver. Cu's easy and quick oxidizing metal nature has prevented it from receiving much attention as a plasmonic material [19,20]. According to recent research by Singh et *al.*, appropriate oxide coatings can prevent the oxidation of copper [21]. Sharma et *al.* proposed that, in addition to keeping copper from oxidizing, using a thin layer of Pt over copper can improve the sensitivity of the SPR sensor [22]. Recently, it was proposed by Rifat et *al.* that a graphene covering over Cu prevents the Cu from oxidation, increasing the sensor's durability and plasmonic performance stability [23]. Myilsamy et *al.* proposed an SPR sensor for 2D materials using Cu and Pt layer produces sensitivity up to 502°/RIU with figure of merit (ZT) as 128.7RIU^{-1} [24]. According to Karki et *al.*, Cu/$BaTiO_3$/BP structure exhibits extraordinarily high sensitivity of 378°/RIU [25]. Many materials have been developed recently to limit oxidation. Graphene, BP, MXene, and transition metal dichalcogenide (TMDC) are examples of 2D materials with significant interest in SPR sensors and have unique optical and electrical properties [26–28]. Graphene has emerged as a novel avenue for increasing the sensitivity of several types of optical sensors. It has been shown that the sensitivity of the detector can be increased by covering a metal with a monolayer of graphene [29]. Graphene has garnered a lot of attention due to its highly fascinating optical, mechanical, and high electron mobility capabilities. Its tunable bandgap, lowest resistivity, and superior biomolecule adsorbent, which all lead to higher SPR sensitivity, and have demonstrated potential [30,31]. As a result, graphene is a superior material for biomolecule adsorption and has the potential to greatly increase the SPR biosensor's efficiency. For instance, a graphene-based SPR biosensor has been successfully used for hemoglobin detection in blood samples, show casing significant sensitivity and precision [32]. SPR phenomena are utilized in the graphene layer to identify gasses [33]. Pal et *al.* report on investigating an SPR sensor designed structure of BK7, silver, platinum, graphene, and magnesium difluoride with an impressive sensitivity of 430 degree/RIU [34]. Verma et *al.* proposed in SPR sensor basic graphene-based design attained high sensitivity of SPR biosensor and achieved as high as 2.35 times in the absence of air gap [35]. Otto comparison was used by Maharana et *al.* to conceptually examine an SPR sensor design, with graphene film serving as the fundamental recognition element (BRE) [36]. Bijalwan et *al.* employed metal layers of Au and Al with graphene (2D-material) Nano layers to find sensitivity as high as 160°/RIU. They also obtained sensitivity of 163°/RIU using a different combination of WSe_2 with Au and Al (bi-metal films) [37]. Karki et *al.* employed graphene and zinc sulfide with Ag in the visible region, reaching a sensitivity of 292°/RIU [38]. Pandey et *al.* analyzed a design SPR sensor using blue phosphorus/MoS_2 heterostructure, attaining a sensitivity of 458°/RIU at the visible wavelength of 662 nm [39]. Similarly, the integration of a bimetallic Cu–Ni structure in 2D material-based SPR sensors enhances sensitivity considerably of about 426°/RIU [40]. Maheswarie et *al.* also reported that addition of BP/Graphene over the bimetallic (Cu–Co) layer, enhances the sensitivity to 504°/RIU [41]. Wang uses black phosphorus and ZnO in an SPR biosensor. It is discovered that the maximum sensitivity is 400°/RIU for the suggested sensing structure [42]. More recently, black phosphorus (BP) has gained attention for its low absorption, faster biomolecular adsorption energy, direct band gap, high mobility, low extinction and its larger molar response factor. Another material causes minimal oxidation even though BP oxidizes quickly because molecule binding works well inside the sensing layer [43,44], combining BP with bilayer WSe_2 on a BK7 prism improves sensitivity up to 279°/RIU [45]. Wu et al. used few-layer black phosphorus-graphene/TMDCs heterostructures with Ag, achieving a sensitivity of 279°/RIU [46]. The other plasmonic material using in our work is halide perovskite ($FASnI_3$). Its optical and electrical properties are remarkable, exhibiting a small band gap and high optical absorption in the visible spectrum with better optoelectronic properties [47]. Roy et al reported that the SPR heterogenous structure based on WS_2, halide perovskite ($FASnI_3$) and BP improved sensitivity and ZT for 402°/RIU and 48.2/RIU, respectively [48]. Malek et al use hybrid organic–inorganic halide perovskites and graphene layers over as reached the sensitivity 298.5°/RIU [49]. Rajeev et al propose as sensor incorporates the BAF10/Cu/perovskite materials/Si/sensing medium (SM) layers, where the sensitivity and figure of merit (ZT) are 348.75°/RIU and 108.11/RIU [50]. On the other hand, the FASnI3 halide perovskite (HP) and 2D black phosphorous (BP) sensor heterostructures demonstrate that covering the Ag layer with MoO_3 can increase the detection accuracy of our primary HP-based SPR biosensor up to 55.6 % [51]. Our schematic diagram-based halide perovskite (FASnI3) and 2D materials like (black phosphorus (BP, MoS_2, $MoSe_2$, WS_2, WSe_2, and graphene) are designed for the detection of normal and cancer breast cells. As parts of the biomolecular recognition system, halide perovskite (FASnI3) and BP cooperate. In this work, the performance of such a device is examined using the transfer matrix technique (TMM). All layer thicknesses are tuned in order to improve sensor performance. The sensitivity of the sensor is greatly increased by incorporating halide perovskite (FASnI3) and 2D materials into the BK7/Cu/sensing medium structure, as shown by the results of our simulation. The suggested SPR biosensor, configured as BK7/Cu (48 nm)/$FASnI_3$ (5 nm)/BP (0.53 nm), demonstrated an impressive sensitivity of 338.45 %, higher than the conventional copper-based sensor.

Theoretical model

Structure of proposed biosensor

The most widely accepted TM-polarized He-Ne laser light with a wavelength of 633 nm coupling method for SPR nanostructures employs a BK7 glass prism with high refractive index and high efficiency. The schematic structure based on the Kretschmann configuration consists of five layers such as BK7 prism, Cu, $FASnI_3$ (halide perovskite), 2D materials layer, and breast cell (normal or cancerous). The thicknesses of the Cu, $FASnI_3$, and 2D materials layers are denoted as d_{cu}, d_{FASnI3}, and d_{BP}, respectively, while the refractive indices are represented by n_{Cu}, n_{FASnI3}, and n_{BP}. Our proposed SPR biosensor is depicted in Fig. 1. The RI of the BK7 glass prism can be calculated using the dispersion equation [52]:

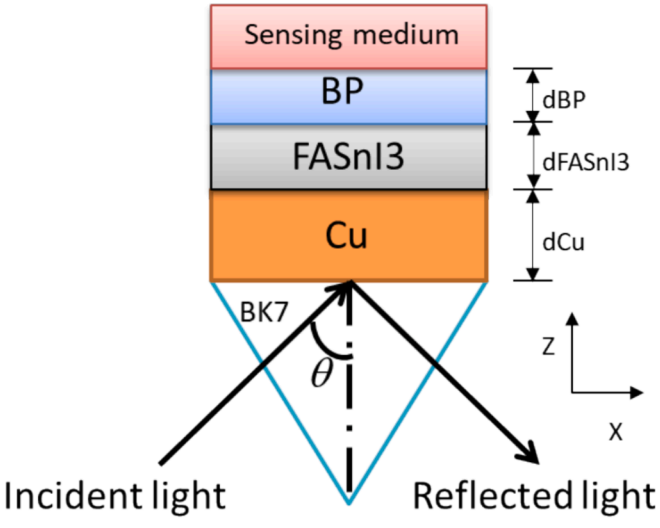

Fig. 1. SPR diagram based on $FASnI_3$-BP layers.

$$n_p = \sqrt{\frac{1.03961212\lambda^2}{\lambda^2 - 0.00600069867} + \frac{0.231792344\lambda^2}{\lambda^2 - 0.0200179144} + \frac{1.03961212\lambda^2}{\lambda^2 - 103.560653} + 1} \quad (1)$$

where λ is the wavelength (μm).

The second layer, is the metal plasmonic copper Cu, which is used in this designed SPR biosensor. The Drude model is used to calculate the dielectric constant of copper, it can be expressed as follows [53]:

$$\varepsilon_{Cu} = 1 - \frac{\lambda^2 \lambda_c}{\lambda_p^2 (\lambda_c + i\lambda)} \quad (2)$$

where $\lambda_c = 4.0852 \times 10^{-5}$m and $\lambda_p = 1.3617 \times 10^{-7}$ m represent the wavelength of collusion and the plasma of copper, respectively. The third layer is halide perovskite ($FASnI_3$), followed by a fourth layer of BP. The thickness and refractive index of the materials used are shown in Table 1. The last layer contains normal (Healthy MDA-MB-231 cell) and cancer breast cells (Cancerous MDA-MB-231 cell) with refractive indices (nSM) of 1.385 and 1.399 in visible range, respectively [54].

Reflectance

The proposed multi-layer SPR biosensor model's light reflection was calculated using the Fresnel equations technique and the transfer matrix method (TMM); the wave parameters for the N-layer architecture that describes the relationship between the tangential field items of each layer from the first in ($Z = Z_{1=0}$) to the last layer ($Z = Z_{N\_1}$) can be symbolized as:" [61].

$$\begin{bmatrix} E_1 \\ H_1 \end{bmatrix} = [M] \times \begin{bmatrix} E_{N-1} \\ H_{N-1} \end{bmatrix} \quad (3)$$

(E_1), (H_1), (E_{N-1}) and (H_{N-1}) represent tangential electromagnetic fields at the first and last layer boundaries, respectively. The characteristic matrix (M) of an N-layer SPR system is given as:

$$M = \prod_{k=1}^{N-1} M_k = \begin{bmatrix} M_{11} & M_{12} \\ M_{21} & M_{22} \end{bmatrix} \quad (4)$$

$$M_k = \begin{bmatrix} \cos\delta_k & \frac{-\sin\delta_k}{q_k} \\ -i q_k \sin\delta_k & \cos\delta_k \end{bmatrix} \quad (5)$$

where δ_k and q_k are the phase factor and the admittance of a specific phase respectively, and both can be determinate by:

$$q_G = \frac{\left(n_k^2 - k_k^2 - n_p^2 \sin^2\theta_i - 2 i n_k k_k\right)^{1/2}}{\varepsilon_k} \quad (6)$$

$$\delta_k = \left(\frac{2\pi}{\lambda}\right) d_k \left(n_k^2 - k_k^2 - n_p^2 \sin^2\theta_i - 2 i n_k k_k\right)^{1/2} \quad (7)$$

θ_i is the incidence angle and n_p is the refractive index of prism, n_k and k_k are the real and imaginary parts part of the dielectric function of N-layer. The equation of reflection coefficient (r_p) and the expression for reflectance (R) are as follows:

$$r_p = \frac{(M_{11} + M_{12} q_N) q_1 - (M_{21} + M_{22} q_N)}{(M_{11} + M_{12} q_N) q_1 + (M_{21} + M_{22} q_N)} \quad (8)$$

$$R_p = |r_p|^2 \quad (9)$$

Performance parameters

SPR sensor performance is evaluated based on parameters such as angular sensitivity (S), detection accuracy (DA), and figure of merit (ZT) to ensure optimal performance [62]. The angular sensitivity (S) is defined as the change in the resonance angle ($d\theta_{SPR}$) caused by the minimum variation in the refractive index of the last layer ($dn_{biosample}$). It is given by [63]:

$$S = \frac{d\theta_{SPR}}{dn_{biosample}} \quad (10)$$

The full width at half maximum (*FWHM*) of the SPR dip in the reflectance curve indicates how sharp the resonance is:

$$FWHM = \theta_2 - \theta_1 \quad (11)$$

where θ_1 and θ_2 are resonance angles at half of the reflectivity SPR curve.

Another important key parameter is detection accuracy (DA), which refers to a sensor's ability to detect small changes in an analyte's refractive index. It is given in the following relationship:

$$DA = \frac{1}{FWHM} \quad (12)$$

Another parameter to consider is the figure of merit (ZT), which is a measure of the sensor's performance defined as the ratio of sensitivity (S) to the FWHM of the SPR curve [64].

$$FOM = \frac{S}{FWHM} ZT = \frac{S}{FWHM} \quad (13)$$

Results and discussion

Effect of prism material on design of SPR biosensor

In this numerical model, we have taken CsF, BK7, BAK1, BAF10 and 2S2G glass prism with refractive index 1.4768, 1.515, 1.570, 1.667, 2.358, respectively [48].

Fig. 2 **(a)** depicts the resonance curves for all prism materials CsF, BK7, BAK1, BAF10 and 2S2G with samples breast cell. Copper film thickness is kept at 48 nm throughout the simulations. The sensitivity as given by equation (10) can be theoretically evaluated using the simulated plots. The sensitivity calculation, Δns of 0.014 is assumed. The effect of CsF, BK7, BAK1, BAF10 and 2S2G prisms on structure 1 is illustrated in Fig. 2, along with the typical performance parameters. From Fig. 2 (a) and 2 (b), it can be realized that BK7 prism outcomes with the best performance among all of the selected prisms having best sensitivity (S) of 459.28∘/RIU and minimum reflectance (Rmin) of 0.0714 (θRmin = 81.77∘). The resonance curves for samples of breast cells for all prism materials CsF, BK7, BAK1, BAF10, and 2S2G are shown in Fig. 2 **(a)**. The thickness of the copper coating is maintained at 48 nm during the simulations. Using the simulated plots, it is theoretically possible to evaluate the sensitivity as provided by equation (10).

A sensitivity computation with Δns of 0.014 is made. Fig. 2 shows the normal performance metrics as well as the impact of CsF, BK7, BAK1, BAF10, and 2S2G prisms on structure 1. The highest performance of all the selected prisms can be found in Fig. 2 **(a)** and 2 (b), where the BK7 prism has the best sensitivity (S) of 459.28∘/RIU and the lowest

Table 1
The ideal material thickness and refractive index for the current biosensor are 633 nm.

Material	Thickness of Monolayer (nm)	Refraction Index	Ref
Prism BK7	–	1.5151	[6]
Cu	48	0.0369 + 4.5393i	[53]
$FASnI_3$	5	2.782	[55]
BP	0.53	3.5 + 0.01i	[56]
MoS_2	0.65	5.08 + 1.723i	[57]
$MoSe_2$	0.70	4.62 + 1.0063i	[58]
WS_2	0.80	4.9 + 0.3124i	[59]
WSe_2	0.70	4.55 + 0.4332i	[25]
Graphene	0.34	3 + 1.1491i	[60]

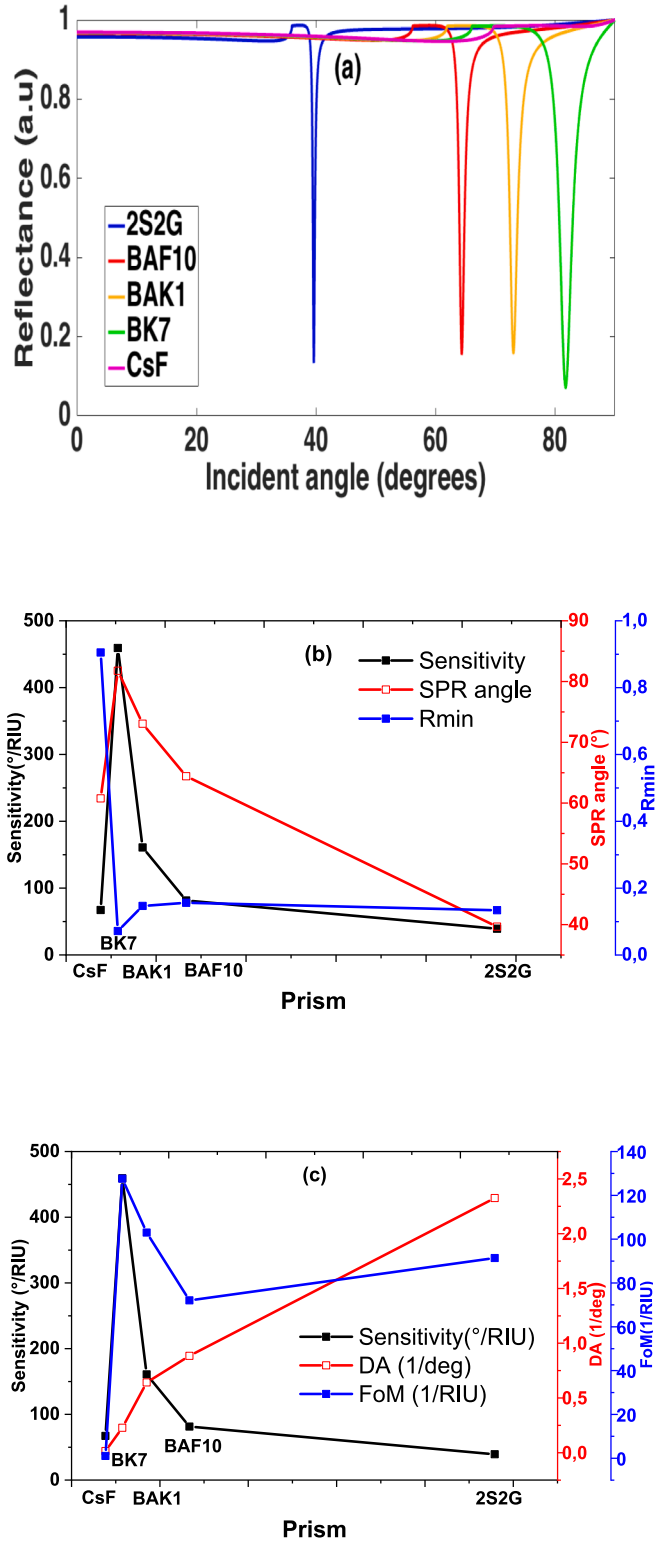

Fig. 2. Reflectance curve with incident angle (a), Angular sensitivity, SPR angle low reflectance (θ_{Rmin}) and minimum reflectance (R_{min}) (b), and sensitivity, DA, ZT for CsF, BK7, BAK1, BAF10 and 2S2G prisms, assuming sensing medium RI 1.385 (c).

reflectance (Rmin) of 0.0714 (θ_{Rmin} = 81.77∘). The optimal values for DA and ZT for the BK7 prism are determined to be 0.227/∘ and 127.57 RIU^{-1}, respectively, based on Fig. 2 **(c)**. It is appropriate for SPR sensors because it provides high transmission, a wide range of optical devices that require low dispersion, and a stable and high refractive index.

Effects of BP and $FASnI_3$ on biosensor performance

The effectiveness of the suggested $FASnI_3$ structure when combined with 2D materials at various SPR biosensor architectures are compared and examined in relation to BP. Table 2 demonstrates the comparison with three conventional sensors, it can be observed that the optimum highest sensitivity and ZT are 459.28°/RIU and 127.57/RIU by using the schematic structure with thickness BK7/Cu(48 nm)/$FASnI_3$(5 nm) /BP (0.53 nm)/sensing medium with RI of normal and cancer breast cell. The proposed construction utilizes the $FASnI_3$ along with the high biomolecule adsorption of BP for sensing performance improvement. Adding the $FASnI_3$ layer to the Kretchmann configuration without the BP layer increases the sensitivity by 329.28°/RIU, indicating that the $FASnI_3$ layer incorporated into the Kretchmann model contributes to achieve the sensitivity enhancement; however, the addition of Black phosphor (BP) in the structure BK7/Cu (48 nm)/$FASnI_3$(5 nm)/sensing medium improves sensitivity and ZT due to the BP's robust interaction with biological sensing medium.

Effect of Cu layer thickness on sensitivity and their optimization

The sensor's sensitivity and ZT were improved as a result of adjusting the Cu layer thickness to obtain the ideal structure parameters for the biosensor. Table 3 demonstrates that as the Cu layer thickness increases in the conventional structure of the SPR biosensor BK7/Cu/$FASnI_3$/BP/sensing medium, the performance parameters also increase. Specifically, the sensitivity rises from 233.57°/RIU to 459.28°/RIU when the Cu thickness goes from 30 nm to 48 nm. It is clear that the optimal Cu layer thickness is 48 nm, which is associated with the maximum S = 459.28°/RIU, ZT = 123.11/RIU, and DA = 0.2732$^{\circ-1}$. The difference in sensitivity, ZT, and DA for various Cu thicknesses are reported in Table 3.

Analysis of performance for various 2D materials

Fig. 3 **(a-f)** depict the reflectivity curves for various SPR models for change in sensing mediums RI between 1.385 and 1.399. The change of resonance angle for divers conventional SPR biosensor with 2D materials is 6.43°, 4.51°, 4.59°, 5.57°, 5.25°, and 5.65° with various structure:

BK7/Cu(48 nm)/$FASnI_3$(5 nm)/BP(0.53 nm); BK7/Cu(35 nm)/$FASnI_3$(5 nm)/MoS_2(0.65 nm);

BK7/Cu(35 nm)/$FASnI_3$(5 nm)/$MoSe_2$(0.7 nm); BK7/Cu(35 nm)/$FASnI_3$(5 nm)/WS_2(0.8 nm);

BK7/Cu(48 nm)/$FASnI_3$(5 nm)/WSe_2(0.7 nm) and BK7/Cu(48 nm)/$FASnI_3$(5 nm)/Graphene (0.34 nm); the sensitivity values for each structure are 459.28°/RIU, 322.14°/RIU, 327.85°/RIU, 397.85°/RIU, 375°/RIU, and 403.57°/RIU, respectively.

The performance parameters of various conventional SPR models for different thicknesses range of copper Cu (30–60 *nm*) by changing the RI 0.014. The sensitivity, ZT, and DA values for each structure are shown in Fig. 4. Initially, in an effort to maximize FoM and increase optimal sensitivity, we looked into adding 2D materials to copper and optimizing copper thickness. For the convective structure BK7/Cu/$FASnI_3$/Graphene/SM, the values of the sensitivity, ZT, and DA at 60 nm thickness of

Table 2
SPR sensor reflectance curve performance characteristics for various structures.

Sensor structure	R_{min}	Sensitivity (°RIU^{-1})	FWHM (°)	DA ($^{\circ-1}$)	FoM (RIU^{-1})
BK7/Cu/sensing medium	0.1578	162.85	1.2	0.8333	135.7
BK7/Cu/$FASnI_3$/ sensing medium	0.0109	329.28	2.79	0.3584	118.02
BK7/Cu/$FASnI_3$/ BP/sensing medium	0.2814	459.28	3.6	0.2777	127.57

Table 3
Performance factors for optimized combination of copper Cu thickness of present SPR.

Cu Thickness (nm)	FASnI3 (nm)	BP (nm)	R_{min}	S (°/RIU)	ZT (1/RIU)	DA ($^{\circ -1}$)
30	5	0.53	0.6794	233.57	37.25	0.1594
30	7	0.53	0.1136	390.71	139.04	0.3355
30	5	0.53	0.618	280.7	45.12	0.160
40	5	0.53	0.8653	267.85	51.31	0.191
35	5	0.53	0.4423	290	57.31	0.1976
40	5	0.53	0.1365	358.57	84.56	0.2358
45	5	0.53	0.0215	437.85	115.83	0.2645
47	5	0.53	0.1677	457.85	126.12	0.2784
48	5	0.53	0.2814	459.28	127.57	0.2777
50	5	0.53	0.506	450.71	123.14	0.2732

Cu are 403.57°/RIU, 49.29/RIU, and 0.2336, respectively. It is noticed that these values rise with the Cu layer. On the other hand, with the outher suggested conventional construction, performance rises until Cu thickness reaches its maximum and then falls. The highest sensitivity and ZT of the conventional structure BK7/Cu/$FASnI_3$/BP/SM optimal performance sensor, with a thickness of 48 nm, are 459.28°/RIU and 127.57/RIU, respectively.

We investigated the usual structures BK7/Cu/$FASnI_3$/MoS2/SM, BK7/Cu/$FASnI_3$/$MoSe_2$/SM, and BK7/Cu/$FASnI_3$/WS_2/SM. At 35 nm thickness of Cu layer, we found the best ZT of approximately 46.61/RIU, 48.78/RIU, and 79.09/RIU, respectively, and the greatest sensitivity of approximately 322.14°/RIU, 327.85°/RIU, and 397.85°/RIU, respectively. Lastly, for the standard multilayer BK7/Cu/$FASnI_3$/WSe_2/SM, the optimal sensitivity and ZT values are 375°/RIU and 73.24/RIU, respectively, at 40 nm of Cu layer.

As a result, the optimized thicknesses of 2D materials BP, MoS_2, $MoSe_2$, WS_2, WSe_2, and graphene provide the best performance. Table 4

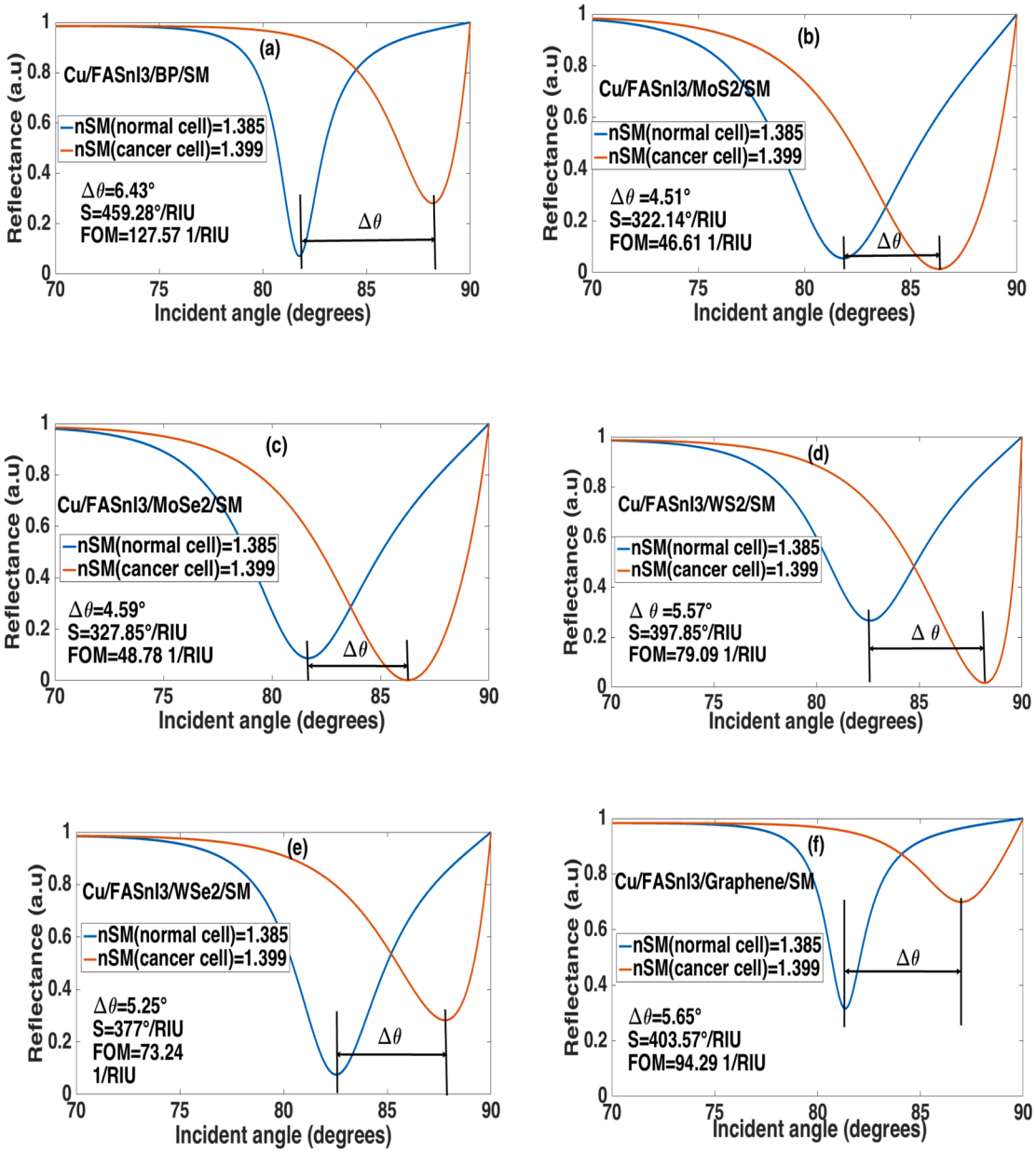

Fig. 3. The reflectance as function of resonance angle incident, BK7/Cu/$FASnI_3$/BP (a), BK7/Cu/$FASnI_3$/MoS_2 (b), BK7/Cu/$FASnI_3$/$MoSe_2$(c), BK7/Cu/$FASnI_3$/WS_2 (d), BK7/Cu/$FASnI_3$/WSe_2 (e) and BK7/Cu/$FASnI_3$/Graphene (f), respectively.

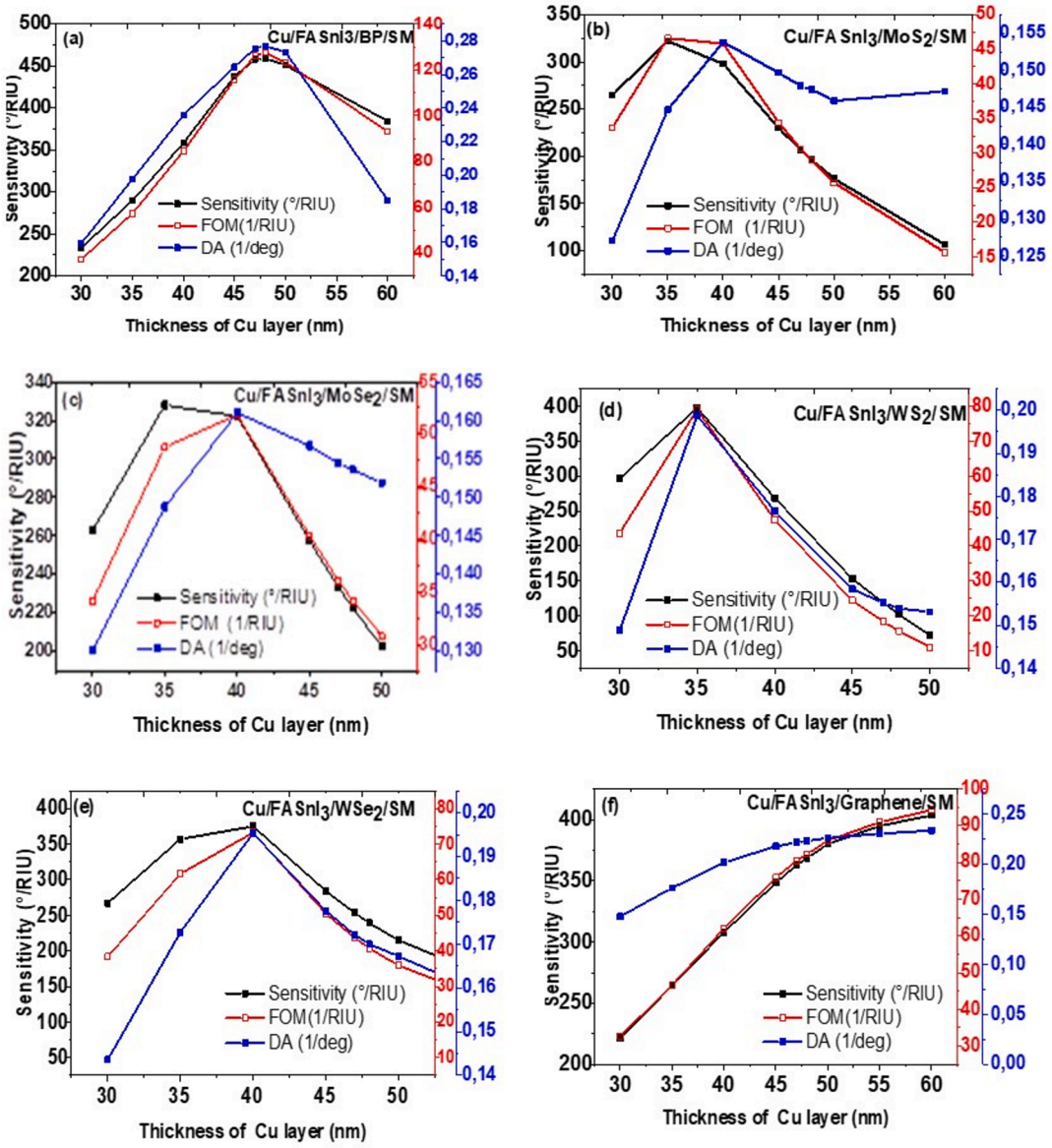

Fig. 4. The variation of S, FoM and DA at optimized thickness of Cu layer at 30 nm-60 nm of BK7/Cu/FASnI$_3$/BP (a), BK7/Cu/FASnI$_3$/MoS$_2$ (b), BK7/Cu/FASnI$_3$/MoSe$_2$ (c), BK7/Cu/FASnI$_3$/WS$_2$ (d) BK7/Cu/FASnI$_3$/WSe$_2$ (e) and BK7/Cu/FASnI$_3$/Graphene (f), respectively.

Table 4
The performance parameters of the SPR biosensor reflectance spectrum for various architectures.

Material	Optimized layers (L)	Thickness of Cu (nm)	S (°/RIU)	ZT(1/RIU)	*DA* ($^{\circ -1}$)
BP	1	48	459.28	127.57	0.2777
MoS2	1	35	322.14	46.61	0.1447
MoSe2	1	35	327.85	48.78	0.1488
WS2	1	35	397.85	79.09	0.1988
WSe2	1	40	375	73.24	0.1953
Graphene	1	60	403.57	94.29	0.2336

shows that the different SPR biosensor structures have good performance parameters.

Enhancement factor for electric field intensity

The electric field distribution displays for the prism BK7/Cu/FASnI3/BP/sensing medium (breast cells) construction as shown in Fig. 5. The probing field intensity is found to be significantly more intense in the sensing medium, and it is seen that the electric field intensity at the interface Cu/FASnI3/BP is amplified and reaches its highest value at the interface of BP and sensing medium. This explains why the SP waves are stronger and appear to be more sensitive. The sensing output of this suggested structure is larger than that of the other structures when compared to previously published studies on SPR sensor construction (see Table 5).

Finally, Table 5 compares some of the current SPR sensors with previously suggested works. The analysis demonstrates that the work being done now improves performance in terms of ZT and sensitivity.

Conclusion

This paper investigates a novel SPR biosensor that uses the BK7 glass prism, metal plasmonic copper Cu, halide perovskite (FASnI$_3$), and 2D materials for the detection of cancerous breast cells. The setup is based on the Kretschmann configuration, and Fresnel equations and the transfer matrix method are used to theoretically analyze it. The attenuation total reflection method was used for the examination of the

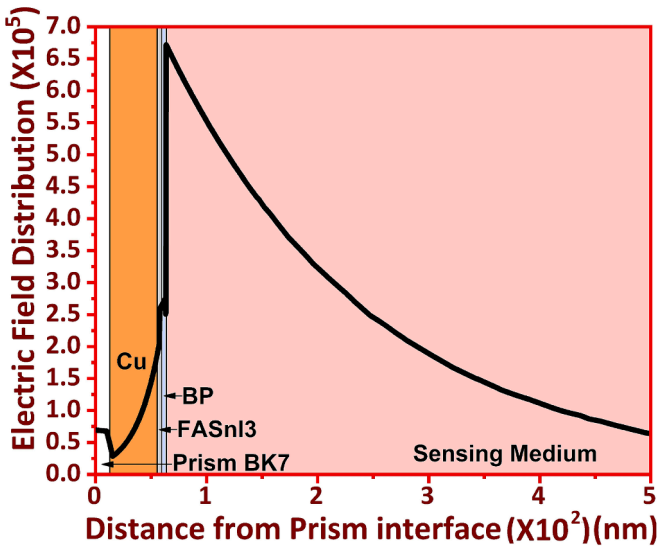

Fig. 5. Electric field distribution as a function of distance from prism interface of BK7/Cu/FASnI3/BP/sensing medium.

Table 5
Comparison of the present sensor with other existing works.

Ref.	Year	Structure	S	DA	ZT
[65]	2024	Prism/Ag/SnS_2/graphene	158	–	–
[66]	2024	Ag/Si/Au/$PtSe_2$	206	0.116	24.03
[67]	2024	CaF_2/$PtSe_2$/Au/BlueP-MoS_2	240.54	0.1215	29.22
[68]	2023	BK7/Ag/$TiSi_2$/BP	257.3	–	–
[60]	2024	BK7/Cr/Au/Si/Graphene/WSe	333.33	0.588	196
[48]	2024	BAK1/Ag/ WS_2/$FASnI_3$/ BP	402	0.27	48.2
[69]	2024	BK7/Ag/Pd/WS_2	409.36	0.180	73.64
[70]	2024	CaF_2/Ag/BaTiO3/WS_2	450	0.285	128.57
[71]	2024	CsF/Ag/Pd/$TaSe_2$	410	0.198	73.873
[72]	2020	CsF/Cu/Ni	426	–	–
Our work	2024	BK7/Cu/$FASnI_3$/BP	459.22	0.2732	123.11

reflection. We evaluated the various configurations of the SPR biosensor to achieve the best performance. It has also been used to optimize the angular sensitivity and other sensor parameters, such as layer thickness and number. We optimized the thickness of $FASnI_3$ and 2D materials (BP, MoS_2, $MoSe_2$, WS_2, WSe_2, and graphene) in the current SPR biosensor to distinguish between normal and cancerous breast cells. Our simulation results show that incorporating 2D materials into the structure BK7/Cu/$FASnI_3$ improves sensitivity. Our proposed SPR's primary performance parameter is its sensitivity of 459.28°/RIU, which we achieved with an achievement of 338.45 % and ZT as high as 123.11/RIU using a configuration structured by BK7/Cu (48 nm)/$FASnI_3$ (5 nm)/BP (0.53 nm). According to the obtained results, the suggested biosensor produces results that are more sensitive than those of previous reports. Our results show that incorporate $FASnI_3$ and *2*D material in SPR biosensors significantly achieved sensitivity and ZT for various sensing applications in diagnostics and biosensing.

CRediT authorship contribution statement

H. Bouandas: Resources, Project administration. **Y. Slimani:** Investigation. **A. Bakhouche:** Formal analysis, Data curation. **N. Bioud:** Investigation, Funding acquisition. **A. Djemli:** Project administration, Methodology. **Faisal Katib Alanazi:** . **I. Bouchama:** Project administration, Methodology. **M.A. Ghebouli:** Methodology, Investigation. **M. Fatmi:** Writing – original draft, Visualization, Validation. **T. Chihi:** Software, Resources.

Declaration of competing interest

The authors declare that they have no known competing financial interests or personal relationships that could have appeared to influence the work reported in this paper.

Data availability

The authors do not have permission to share data.

Acknowledgment

The authors extend their appreciation to the Deanship of Scientific Research at Northern Border University, Arar, KSA for funding this research work through the project number NBU-FFR-2024-310-04

References

[1] Homola J, Yee SS, Gauglitz G. Surface plasmon resonance sensors. Springer Sens Actuators, B Chem 1999;54:3–15.
[2] Raghuwanshi SK, Pandey PS. A numerical study of different metal and prism choices in the surface plasmon resonance biosensor chip for human blood group identification. IEEE Trans NanoBiosci 2023;22(2):292–300.
[3] Kumar V, Raghuwanshi SK, Kumar S. Novel surface plasmon resonance (SPR)-based biosensor for pathogenic bacteria detection (PathoBactD). Opt Interact Tissue Cells XXXV 2024;12840:14–20.
[4] Salah NH, Pal A, Rasul HM, Uniyal A. Sensitivity enhancement of the surface plasmon resonance sensor based on gallium doped zinc oxide and silicon for cancer detection: a wavelength interrogation approach, micro and nanostructures. Springer Micro Nanostruct 2024;186:207736.
[5] Nagarajan P, Manoharadas S, Dhasarathan V, Rajeshkannan S. Cancer detection using multilayered kretschmann configuration–based refractive index sensor. Plasmonics 2024;18:1.
[6] Elsayed HA, Awasthi SK, Almawgani AHM, Mehaney A, Ali YAA, Alzahrani A, et al. High-performance biosensors based on angular plasmonic of a multilayer design: new materials for enhancing sensitivity of one-dimensional designs. RSC Adv 2024;14(11):7877–90.
[7] Otto A. Excitation of Nonradiative surface plasma waves in silver by the method of frustrated total reflection. Springer Zeitschrift Für Phys 1968;216:398–410.
[8] Kretschmann E, Raether H. Radiative decay of non-radiative surface plasmons by light. Springer z Naturforsch 1968;23:2135–6.
[9] Sharma AK, Kaur B, Popescu VA. On the role of different 2D materials/heterostructures in fiber-optic SPR humidity sensor in visible spectral region. Springer Opt Mater (Amst) 2020;102. 109824.
[10] Sohrabi F, Hamidi SM. Neuroplasmonics: From Kretschmann configuration to plasmonic crystals. Eur Phys J plus 2016;131:221.
[11] Cai D, Lu Y, Lin K, Wang P, Ming H. Improving the sensitivity of SPR sensors by double-dips method (DDM). Opt Express 2008;16:14597.
[12] Lee M, Jeon H, Kim S. A highly tunable and fully biocompatible silk nanoplasmonic optical sensor. Springer Nano Lett 2015;15:3358–63.
[13] Kumar V, Raghuwanshi SK, Kumar S. Realization of prism-based surface plasmon resonance sensor for detection of methane gas, oxide-based materials and devices XIV. SPIE Proc 2024;12422:73–80.
[14] West PR, Ishii S, Naik GV, Emani NK, Shalaev VM, Boltasseva A. Searching for better plasmonic materials. Springer Laser Photon Rev 2010;4:795–808.
[15] Naik GV, Shalaev VM, Boltasseva A. Alternative plasmonic materials: beyond gold and silver. Adv Mater 2013.
[16] Hakami J, Abassi A, Dhibi A. Performance enhancement of surface plasmon resonance sensor based on Ag-TiO_2-$MAPbX_3$-graphene for the detection of glucose in water. Opt Quant Electron 2021;53:1.
[17] Ong BH, Yuan X, Tjin SC, Zhang J, Ng HM. Optimised film thickness for maximum evanescent field enhancement of a bimetallic film surface plasmon resonance biosensor. Sens Actuators B 2006;114(2):1028–34.
[18] Wang S, Liu N, Cheng Q, Pang B, Lv J. Surface plasmon resonance on the antimonene–Fe2O3–copper layer for optical attenuated total reflection spectroscopic application. Plasmonics 2021;16:559–66.
[19] West PR, Ishii S, Naik GV, Emani NK, Shalaev VM, Boltasseva A. Searching for better plasmonic materials. Springer Laser Photon Rev 2010;4(6):795–808.
[20] Masaru M, Miyashita K, Higo M. Sensor properties and surface characterization of the metal-deposited SPR optical fiber sensors with Au, Ag, Cu, and Al. Sensors Actuat A: Phys 2006;125:296–303.
[21] Singh Raman RK, Chakraborty Banerjee P, Lobo DE, Gullapalli H, Sumandasa M, Kumar A, et al. Protecting copper from electrochemical degradation by graphene coating. Carbon 2012;50:4040–5.
[22] Sharma NK, Shukla S, Sajal V. Surface plasmon resonance-based fiber optic sensor using an additional layer of platinum: a theoretical study. Optik 2017;133:43–50.
[23] Rifat AAGA, Mahdiraji R, Ahmed DM, Chow YM, Sua YG, Shee F, Adikan M. Copper-graphene-based photonic crystal fiber plasmonic biosensor. IEEE Photon J 2015;8(1):1–8.

[24] Myilsamy M, Lordwin PC, Vibisha A, Ponnan S, Z.J., Balasundaram RK. Theoretical analysis of a high-performance surface plasmon resonance biosensor using BlueP/WS2 over Cu-Pt bimetallic layer. Photon Lett Poland 2023;15(2):18–20.
[25] Karki B, Pal A, Singh Y, Sharma S. Sensitivity enhancement of surface plasmon resonance sensor using 2D material barium titanate and black phosphorus over the bimetallic layer of Au, Ag, and Cu. Opt Commun 2022;508:127616.
[26] Dutta K, Datta A, Majumder S. Design of plasmonic solar photocatalyst: judicially coupled hot carrier induced surface plasmon of Ag with graphene. Opt Mater 2022;123:111887.
[27] Varghese SS, Varghese SH, Swaminathan S, Singh KK, Mittal V. Two-dimensional materials for sensing: graphene and beyond. Electronics 2015;4(3):651–87.
[28] Fatolahi L, Alemi S, Al-Delf MN, Athab AH, Janani BJ. Optical detection of fat and adulterants concentration milk using TMDC (WS2 and MoS2)-surface plasmon resonance sensor via high sensitivity and detection accuracy. Opt Mater 2024;147:114723.
[29] Mudgal N, Yupapin P, Ali J, et al. BaTiO3-graphene-affinity layer–based surface plasmon resonance (SPR) biosensor for pseudomonas bacterial detection. Plasmonics 2020;15:1221–9.
[30] Jaiswal SK, Maurya JB. Polychromatic behavior of reflectance and field performance of graphene coated SPR sensor. In: Advances in VLSI, Communication, and Signal Processing: Select Proceedings of VCAS 2021. Singapore: Springer Nature Singapore; 2022. p. 435–44.
[31] Laref A, Alsagri M, Alay-e-Abbas SM, Laref S, Huang HM, Xiong YC, et al. and Wu, Electronic structure and optical characteristics of AA stacked bilayer graphene: A first principles calculations. Optik 2020;206:163755.
[32] Karki B, Vasudevan B, Uniyal A, Srivastava V. Hemoglobin detection in blood samples using a graphene-based surface plasmon biosensor. Res Square 2022.
[33] Kumar V, Kumar Raghuwanshi S, Kumar S. Realization of prism-based surface plasmon resonance sensor for detection of methane gas. 12422. Oxide-based Materials and Devices XIV. SPIE; 2023.
[34] Pal A, Trabelsi Y, Sarkar P, Yadav RB, Sharma M, Uniyal A, et al. Plasmonic pregnancy detector: enhancing sensitivity with SPR sensor. Opt Quant Electron 2024;56(9):1404.
[35] Verma A, Prakash A, Tripathi R. Sensitivity enhancement of surface plasmon resonance biosensor using graphene and air gap. Opt Commun 2015;357:106–12.
[36] Maharana PK, Jha R, Palei S. Sensitivity enhancement by air mediated graphene multilayer-based surface plasmon resonance biosensor for near infrared. Sens Actuators B 2014;190:494–501.
[37] Bijalwan A, Singh BK, Rastogi V. Surface plasmon resonance-based sensors using nano-ribbons of graphene and WSe2. Plasmonics 2020;15(4):1015.
[38] Karki B, Uniyal A, Chauhan B, Pal A. Sensitivity enhancement of a graphene, zinc sulfide-based surface plasmon resonance biosensor with an Ag metal configuration in the visible region. J Comput Electron 2022;21:445.
[39] Pandey P, Raghuwanshi SK. Sensitivity enhancement of surface plasmon resonance (SPR) sensor assisted by BlueP/MoS_2 based composite heterostructure. IEEE Access 2022;10:116152–9.
[40] AlaguVibisha G, et al. Sensitivity enhancement of surface plasmon resonance sensor using hybrid configuration of 2D materials over bimetallic layer of Cu–Ni. Opt Commun 2020;463:125337.
[41] Maheswari P, Ravi V, Rajesh KB, Jha R. High Performance bimetallic (Cu-Co) surface plasmon resonance sensor using hybrid configuration of 2D materials. J Environ Nanotechnol 2022;11(3):1.
[42] Wang S, Zhang J, Liu N, Wan J. Sensitivity improvement of bimetallic layer-based SPR biosensor using ZnO and black phosphorus. Plasmonics 2023;18(5):1873–83.
[43] Cho SY, Cho SY, Lee Y, Koh H, Jung H, Kim J, et al. Superior chemical sensing performance of black phosphorus: comparison with MoS_2 and graphene. Adv Mater 2016;28(32):7020–8.
[44] Mao N, Tang J, Xie L, Wu J, Han B, Lin J, et al. Optical anisotropy of black phosphorus in the visible regime. Am Chem Soc 2016;138:300–5.
[45] Wu L, Guo J, Wang Q, Lu S, Dai X, Xiang Y, et al. Sensitivity enhancement by using few-layer black phosphor-rusgraphene/TMDCs heterostructure in surface plasmon resonance biochemical sensor. Sens Actuators B 2017;249:542–8.
[46] Wu L, Guo J, Wang Q, Lu S, Dai X, Xiang Y, et al. Sensitivity enhancement by using few-layer black phosphorus-graphene/TMDCs heterostructure in surface plasmon resonance biochemical sensor. Sens Actuators B 2017;249:542–8.
[47] Obila JO, Lei H, Ayieta E, Ogacho A, Aduda B, Wang F. Optoelectronic property refinement of FASnI3 films for photovoltaic application. Mater Lett 2021;300:130099.
[48] Roy S, Mondol N, Kundu D, Meem AA, Islam MR, Hossain MA, et al. Numerical investigation into impact of halide perovskite material on the optical performance of prism-loaded hybrid surface plasmon resonance biosensor: A strategy to increase sensitivity. Sens Bio-Sens Res 2024;43:100630.
[49] Daher MG, Trabelsi YA, Nacer M, Prajapati YK, Sorathiya VSH, Ahammad, Rashed ANZ. Detection of basal cancer cells using photodetector based on a novel surface plasmon resonance nanostructure employing perovskite layer with an ultra-high sensitivity. Plasmonics 2022;17:2365–73.
[50] Kumar R, Trabelsi Y, Garia L, Kakar VK, Pal A. Halide Perovskite and few-layer silicon-based Surface plasmon resonance sensor for the detection of chemical and biochemical sensing. Phys Scr 2024;99:095543.
[51] Kundu D, Roy S, Mustak R, Eid MM, Rashed ANZ, Mondol N, et al. Feasibility of halide perovskite material-based hybrid surface plasmon resonance biosensor for formalin detection: a numerical investigation. Plasmonics 2024;18:1–17.
[52] Fox M. Optical Properties of solids. Oxford University Press, 3; 2010.
[53] Ordal MA, Long LL, Bell RJ, Bell SE, Bell RR, Alexander RW, et al. Optical properties of the metals Al Co, Cu, Au, Fe, Pb, Ni, Pd, Pt, Ag, Ti, and W in the infrared and far infrared. Appl Opt 1985;22(7):1099–119.
[54] Karki B, Uniyal A, Pal A, Srivastava V. Advances in surface plasmon resonance-based biosensor technologies for cancer cell detection. Internat J Opt 2022;1:1476254.
[55] Seok SI, Guo TF. Halide perovskite materials and devices. MRS Bull 2020;45(6):427–30.
[56] Peng Q, Wang Z, Sa B, Wu B, Sun Z. Electronic structures and enhanced optical properties of blue phosphorene/transition metal dichalcogenides van der Waals heterostructures. Sci Rep 2016;6:1–10.
[57] Shivangani MF, Alotaibi Y, Al-Hadeethi P, Lohia SS, Dwivedi DK, Umar A, et al. Numerical Study to Enhance the Sensitivity of a Surface Plasmon Resonance Sensor with BlueP/WS(2)-Covered Al(2)O(3)-Nickel Nanofilms. Nanomaterials 2022;12:2205.
[58] Alagdar M, Yousif B, Areed NF, Elzalabani M. Improved the quality factor and sensitivity of a surface plasmon resonance sensor with transition metal dichalcogenide 2D nanomaterials. J Nanopart Res 2020;22:1–13.
[59] Das CM, Ouyang Q, Kang L, Guo Y, Dinh XQ, Coquet P, et al. Augmenting sensitivity of surface plasmon resonance (SPR) sensors with the aid of anti-reflective coatings (ARCs). Photon Nanostruct Fund Appl 2020;38:100760.
[60] Salehnezhad Z, Soroosh M, Mondal H. A highly sensitive plasmonic graphene-based structure for deoxyribonucleic acid detection. Photonics 2024;11:6.
[61] Pal S, Verma A, Saini JP, Prajapati YK. Sensitivity enhancement using silicon-black phosphorus-tdmc coated surface plasmon resonance biosensor. IET Optoelectron 2019;13(4):196–201.
[62] Bouandas H, Chorfi H, Ayadi K. Study of human colorectal mucosa by SPR biosensor using admittance loci method. Optik 2021;225:165809.
[63] Basak C, Hosain MK, Sazzad AA. Design and simulation of a high sensitive surface plasmon resonance biosensor for detection of biomolecules. Sensing Imaging 2020;21:1–19.
[64] Pal S, Prajapati YK, Saini JP. Influence of graphene's chemical potential on SPR biosensor using ZnO for DNA hybridization. Opt Rev 2020;27(1):57–64.
[65] Alsaad AM, Al-Hmoud M, Marashdeh MW, Tolstik E, Houshmand M, Telfah A. Highly sensitive silver/tin selenide/graphene multilayer SPR sensor for hemoglobin and glucose levels monitoring in biological fluids. Plasmonics 2024;1–10.
[66] Bouandas H, Slimani Y, Ayadi K, Ghebouli MA, Djemli A, Fatmi M, et al. Sensitivity enhancement of biosensor (SPR) with PtSe2 using Au–Si–Au thin films. J Opt 2024;54:1–9.
[67] Chowdhury AS, Islam MA, Islam MS, Dey B, Park J. Design and analysis of PtSe2 and Blue phosphorus/MoS2 heterostructure-based SPR biosensor. ACS Appl Opt Mater 2024;2.
[68] Almawgani AH, Sarkar P, Pal A, Srivastava G, Uniyal A, Alhawari AR, et al. Titanium disilicide, black phosphorus–based surface plasmon resonance sensor for dengue detection. Plasmonics 2023;18:1223–32.
[69] Fatolahi L, Addulrahman TS, Alemi S, Al-Delfi MN, Athab AH, Janani BJ. Optical detection of fat and adulterants concentration in milk using TMDC (WS2 and MoS2)-surface plasmon resonance sensor via high sensitivity and detection accuracy. Opt Mater 2024;147.
[70] Bhatt S, Bose N, Shushama KN, Inum R, Hasan KBM. Surface plasmon resonance biosensor with high sensitivity for detecting SARS-CoV-2. Plasmonics 2024;19:1–11.
[71] Bouandas H, Slimani Y, Katib Alanazi F, Fatmi M, Chihi T, Djemli A. Detection of tuberculosis using palladium-tantalum diselenide (Pd-TaSe2) based SPR biosensor. J Opt 2024;54:1–8.
[72] AlaguVibisha G, Nayak JK, Maheswari P, Priyadharsini N, Nisha A, Jaroszewicz Z, Jha. Sensitivity enhancement of surface plasmon resonance sensor using hybrid configuration of 2D materials over bimetallic layer of Cu–Ni. Opt Commun 2020;463:125337.